Estimation of External Force Acting on Steel Pile of Steel Pile Reinforced Breakwater

Koyo HIKICHI
Graduate Student, Department of Civil Engineering, Graduate School of Tokyo University of Science, Noda, Japan.
Yoshiaki KIKUCHI
Professor, Department of Civil Engineering, Tokyo University of Science, Noda, Japan.
Taichi HYODO
Associate Professor, Department of Civil Engineering, Tokyo University of Science, Noda, Japan.
Atsushi MOHRI
Graduate Student, Department of Civil Engineering, Graduate School of Tokyo University of Science, Noda, Japan.
Email: 7617618@ed.tus.ac.jp
Keiichi AKITA
University Student, Department of Civil Engineering, Tokyo University of Science, Noda, Japan.
Naoki SHOJI
University Student, Department of Civil Engineering, Tokyo University of Science, Noda, Japan.
Shinji TAENAKA
Senior Researcher, Department of Steel Research Laboratories, Nippon Steel & Sumitomo Metal Corporation, Futtsu, Japan.
Shunsuke MORIYASU
Senior Researcher, Department of Steel Research Laboratories, Nippon Steel & Sumitomo Metal Corporation, Futtsu, Japan.
Shin OIKAWA
Manager, Department of Construction Products Development Div, Nippon Steel & Sumitomo Metal Corporation, Chiyoda, Japan.

ABSTRACT

The coastal areas of the Pacific Ocean suffered extensive damage by the tsunami of the 2011 off the Pacific Coast of Tohoku Earthquake. Then, there are needs to develop reinforcement methods of existing caisson type breakwaters against tsunami force. Installing a row of piles behind the caisson with backfilling, the space between the caisson and piles with rubbles is proposed as one of the reinforcing methods against tsunami. In order to establish the design method of this reinforcing method, the design of the steel pile is the most important. For designing steel piles, it is necessary to estimate the load acting on them from the caisson side. Here, a series of model loading experiments were conducted. The experimental results suggested that the external force acts on the pile only in the ground at the initial stage of loading and it was found that the external forces acting on the piles dominate in the vicinity of the backfilling part by gradually compressing the backfilling part by displacement of the caisson.

Key words: *break water, steel pile, reinforcement, subgrade reaction, tsunami*

1. Introduction

The coastal areas of the Pacific Ocean suffered extensive damage by the tsunami of the 2011 off the Pacific Coast of Tohoku Earthquake. In particular, many breakwaters that had kept the port facilities safe were damaged. Under these circumstances, rebuilding design concept is required. Moreover, it has been predicted with a high probability that the Tonankai, the Nankai Trough earthquake might occur in near future. Therefore, the port structures are strongly required to be strengthened against large tsunamis, by reinforcing the existing caisson breakwaters more than ever. Therefore, by constructing breakwaters that "have toughness" against the tsunami, it is conceivable to make it possible to protect as many people as possible when a huge tsunami occurs.

In order to improve performance of breakwaters against tsunami, Moriyasu *et al*. proposed a method to reinforce a breakwater by installing steel pipe piles behind the breakwater and then filling the space between them using aggregates as shown in **Fig. 1** (Kikuchi *et al*., 2015). This reinforcement method intends to effectively use the resistant behavior of the ground by using steel piles. It has been confirmed that this reinforcing method has high resistance against horizontal force during horizontal loading and hydraulic flume experiments (Arikawa *et al.*, 2015). In order to improve the accuracy of design method of this structure, it is necessary to estimate the external load received from the caisson side of the steel pipe pile in detail, and to check the maximum bending moment responding to actions of external force.

Here, a series of model loading experiments were conducted. The influence of the steel pile on the external load distribution received from the caisson side, and the effect of the maximum bending moment generated in the pile when receiving external loads were experimentally investigated with different number of steel piles.

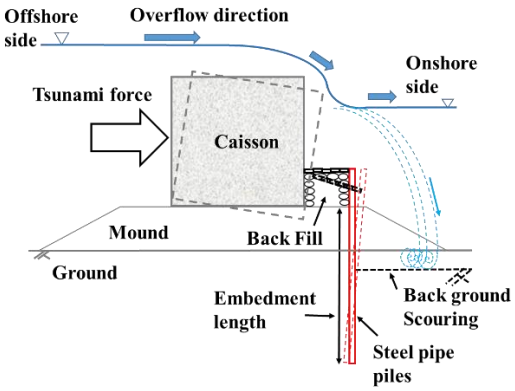

Fig. 1 Schematic diagram of a reinforced gravity type breakwater

2. Experiment outline

In this study, a series of model loading experiments were conducted by changing the spacing between the steel piles behind the caisson. This schematic diagram of the model set up is shown in **Fig. 2**.

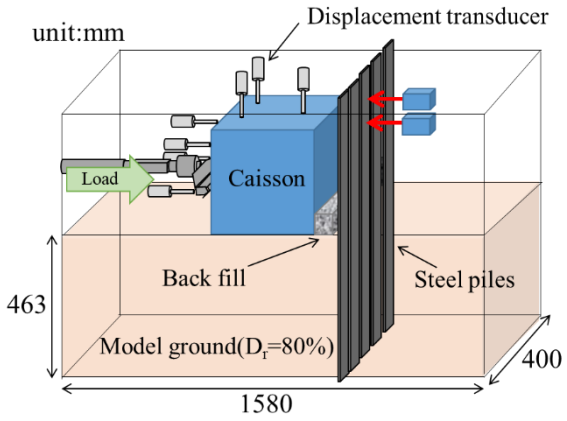

Fig. 2 Schematic diagram of the experimental model set up

The experiment model was designed at 1/60 scale according to similitude shown in **Table 1** (Iai, 1988). A steel sand box of 1580 mm long, 800 mm high and 400 mm wide was used to prepare the model ground as shown in **Fig. 2**. Dry silica sand #5 (D_{50} = 0.591 mm, G_s = 2.647, e_{max} = 1.072, e_{min} = 0.689) was used to prepare the model ground. The model ground was prepared with 80% of relative density by the air pluviation method. The steel piles (800 mm long, 30 mm wide, 2.3 mm thick, flexural rigidity EI = 6.24×10^3 kNmm^2, 463 mm penetration depth) modelling a steel pipe pile were set at a position separated 50 mm from the back of the caisson (380 mm long, 300 mm high, 300 mm wide, γ_t = 22 kN/m^3). Here, experiments were carried on with changing a center to center distance of the piles. A center to center distance of the piles was selected from 120 mm, 60 mm, 33 mm, and the number of piles corresponding to 3, 6, and 12, respectively. **Table 2** shows the experiment cases. A backfill of 50 mm height was installed between the caisson and the steel pile. The material for the backfill was gravel of D_{50} of about 10 mm (G_s was about 2.65, γ_d was

12.1 kN/m^3). A Teflon sheet was affixed to the loading surface of the caisson model to reduce friction. On the bottom of the caisson, sandpaper #150 was attached. Friction was reduced by using a Teflon sheet and a membrane on the contact surface between the ground and the sand box. In the loading experiments, a horizontal load assuming a tsunami wave force was applied. The horizontal load was applied under displacement control at the height of 150 mm, and the monotonous loading speed was at 1 mm / min.

Horizontal displacement of the caisson was measured using LVDTs, fixed at 4 points on the load surface and 3 points on the upper surface. For the piles at the center and side end, as shown in **Fig. 3**, 20 strain gauges were attached to both sides of the pile in the depth direction, and the bending strains were measured.

Table 1. Similarity ratio (Iai,1988)

Items(λ =60)	Prototype/model
Density	1
Acceleration	1
Ground strain	$1/\lambda^{1/2}$
Time	$1/\lambda^{3/4}$
Length	$1/\lambda$
Effective stress	$1/\lambda$
Ground displacement	$1/\lambda^{3/2}$
Bending moment	$1/\lambda^{3}$
Flexural rigidity	$1/\lambda^{7/2}$

Table 2. The details of test conditions.

Number of piles	Center to center distance of piles, l (mm)	Embedded length of pile L (mm)	Total flexural rigidity, EI ($\times 10^4$kNmm^2)
3	120	463	1.87
6	60		3.74
12	33		7.48

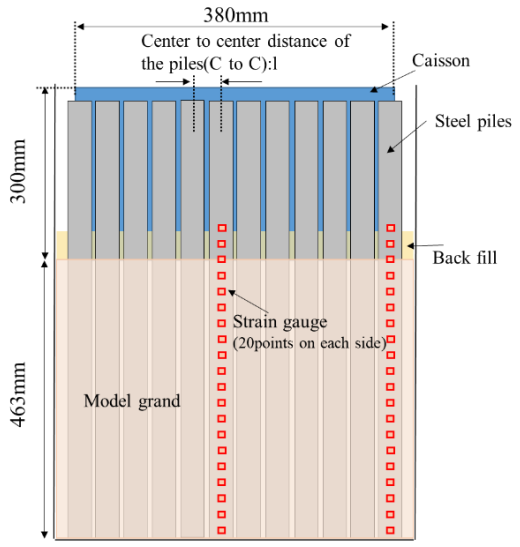

Fig. 3 Schematic diagram of the experimental model set up.(the view from the rear of the caisson.)

3. Experimental results

Fig. 4 shows the relationship between horizontal load and displacement at the center of the caisson in each case. It is understood that the resistance of the caisson decreases by decreasing the number of piles. However, until the horizontal displacement of the caisson gravity center reached 25 mm, there was almost no difference in resistance between 6 and 12 piles.

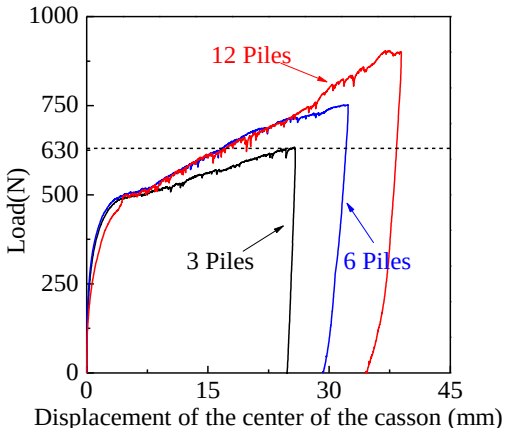

Fig. 4 Relationships of load and the displacement at the center of the caisson under various number of the steel piles.

Fig. 5 shows the bending moment distribution of the center pile in each case at the load of 630N. The bending moment distribution was obtained by approximation using the spline function from the bending moment calculated by strain gauges. As shown in **Fig. 5**, as the number of piles decreases, there is a difference in the load handled by one pile, so the smaller the number of piles is, the larger the maximum bending moment becomes.

Fig. 6 shows the deflection distribution obtained by second-order integration of the bending moment distribution in **Fig. 5** by the bending stiffness EI of the pile. **Fig. 7** shows the load distribution acting on one pile found by second-order differentiation of the bending moment distribution in **Fig. 5**. This load distribution is the difference of the loads acting on both sides of the pile, and they cannot be separated. Therefore, with respect to the subgrade reaction acting on the steel piles acting on the

passive side of the pile, assuming the PHRI method of type S model shown in **Eq. (1)**, and the coefficient of subgrade reaction called k_s required at this time was separately estimated by pile loading experiments (Kubo, 1964).

$$p = k_s \cdot x \cdot y^{0.5} \quad (1)$$

where k_s: coefficient of subgrade reaction (kN/m$^{3.5}$), x: depth(m), y: deflection of steel pile at depth x (m), p: subgrade reaction per unit width at depth x (kN/m^2).

Since k_s is influenced by pile width and ground rigidity, the conditions of the pile (rigidity, number of piles, center pile spacing) and the ground preparation method were set similarly to those of the caisson experiment and statically loaded with a loading height of 60 mm.

Fig. 8 shows the relationship between the pile head load acting per pile and the ground surface displacement in the pile head horizontal loading experiment. The pile head load acting per pile was determined from the slope of the bending moment above the ground by measuring the bending moment by the strain gauge attached to the aerial part and the ground surface. As you can see from this figure, the pile head load acting per pile turns large when the ground surface displacement is equal by reducing the number of piles. However, until the ground surface displacement reached 3 mm, there was almost no difference in the load acting on 3 piles and 6 piles.

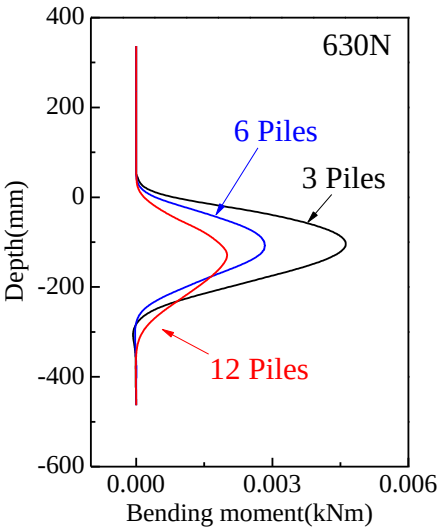

Fig. 5 Bending moment distribution under various number of the steel piles at the horizontal load of 630N

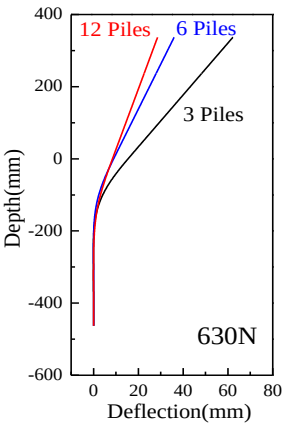

Fig. 6 Deflection distribution under various number of the steel piles at the horizontal load of 630N

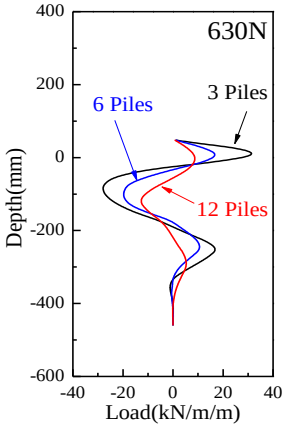

Fig. 7 Load distribution under various number of the steel piles at the horizontal load of 630N

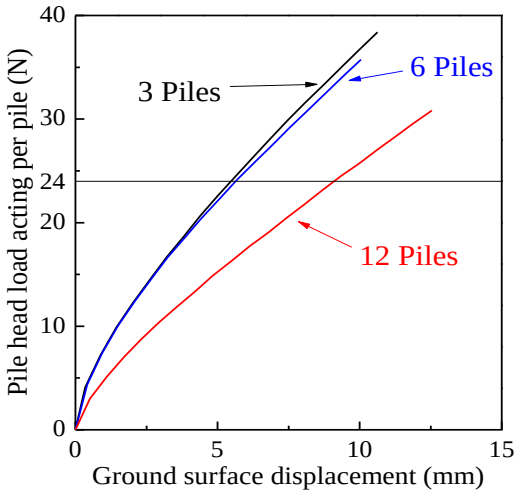

Fig. 8 Relationship between the pile head load acting per pile and the ground surface displacement in the pile head horizontal loading test.

From the relationship between the pile head load and the ground surface displacement shown in **Fig. 8**, k_s as the whole ground was obtained based on the PHRI method of type S model. The relationship between k_s and the ground surface displacement is shown in **Fig. 9**. From **Fig. 9**, it is observed that the initial k_s matches for 3 and 6 piles but the k_s with 6 piles at the ground surface displacement of 3 mm is slightly smaller. The reason is inferred as the influence of the group pile effect in the case of 6 piles, because the receiving area of the adjacent pile interfered. In the case of 12 piles, k_s has a small value from the beginning. This is because the influence of the group pile works immediately after loading as the pile center interval

is very narrow.

In **Fig. 9**, k_s represents the overall behavior of the pile. However, k_s is not constant in the depth direction. Therefore, k_s was estimated from the subgrade reaction and deflection based on the measured values at each depth.

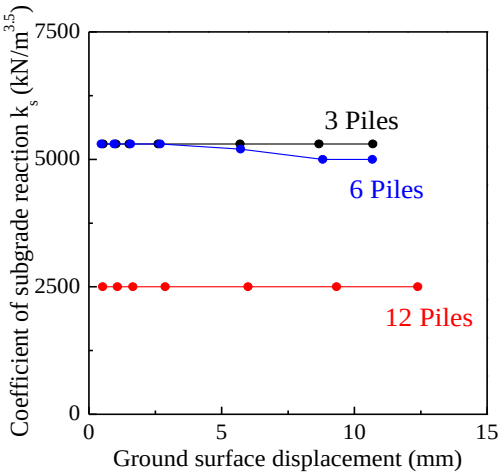

Fig. 9 Relationship between k_s and ground surface displacement

Fig. 10 shows the subgrade reaction distribution based on the bending moment of the actual measurement value when the pile head load acting on one pile is 24N under 12 piles and the subgrade reaction distribution by the PHRI method of type S model when k_s is constant along the depth. In addition, k_s in the PHRI method of type S model was set to 2500 (kN/m $^{3.5}$) from the result in **Fig. 9**. At this time, the maximum bending moment generated at depth $l_{m,\,max}$ was -93 mm. In order to be consistent with the actually measured subgrade reaction distribution, k_s from the ground surface to $l_{m,\,max}$ is k_{s0} and k_s / k_{s0} is shown in relation to the normalized depth x / $l_{m,\,max}$ in the **Fig. 11**. The conditions of other piles (number of piles, pile center spacing), was also examined load conditions, regardless of the load level in PHRI method of type S subgrade reaction model, at a depth from the ground surface $l_{m,\,max}$, subgrade reaction can express with high accuracy with constant k_s. However, for depths beyond $l_{m,\,max}$, unless k_s is varied according to **Fig. 11**, the result is not consistent with the estimate.

The distribution of external forces at 3, 6, and 12 piles in the series of model loading experiments was examined. **Fig. 12** shows the subgrade reaction distribution calculated from the coefficient of subgrade

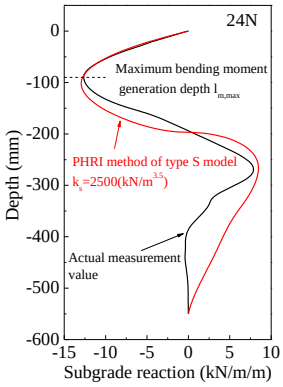

Fig. 10 Subgrade reaction distribution in the pile head horizontal loading test

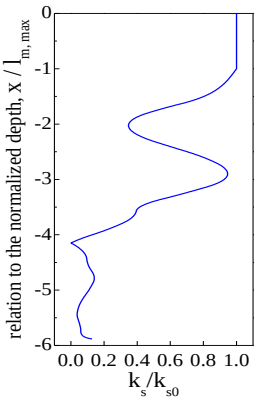

Fig. 11 Change model of the coefficient of subgrade reaction for each depth

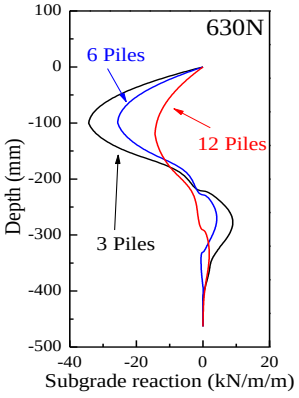

Fig. 12 Subgrade reaction distribution under various number of the steel piles. (Horizontal load of 630N)

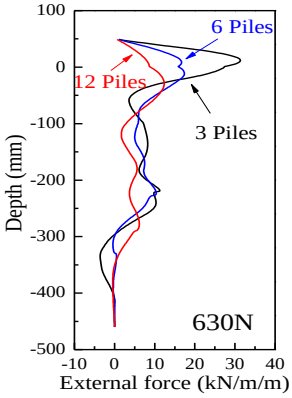

Fig. 13 The external force distribution under various number of the steel piles. (Horizontal load of 630N)

reaction shown in **Figs. 9** and **11** and the deflection distribution shown in **Fig. 6**. Here, from the results in **Fig. 9**, the values of k_{s0} for 3, 6, and 12 piles are set to 5300, 5000, and 2500 (kN / m $^{3.5}$), respectively. **Fig. 13** shows the external force distribution from the caisson side acting on one pile at a loaded load of 630 N, which is obtained by subtracting the load distribution in **Fig. 7** and the subgrade reaction distribution in **Fig. 12**. Looking at the external force distribution, it is understood that in each case the external force acting in the vicinity of the depth of 50 mm to -100 mm is larger than the depth of -100 mm or more. In addition, it can be seen that the magnitude of the external force distribution in each case does not change very much at a depth of more than -100 mm. Comparing each case with a depth of 50 mm to -100 mm, it can be

seen that the smaller the number of piles is, the larger the external force acting from the vicinity of the back-in portion becomes.

The resultant force of the external force distribution acting on all the piles estimated as the loading load was compared (**Table 3**). Since the external force distribution shown in **Fig. 13** is the external force distribution per pile in the center part, the resultant force of the external force multiplied by the number of each pile was used. In the case of 12 piles with a very narrow pile center spacing, the resultant force of the estimated external force was 715 N against the loaded load 630 N. In the case of three piles and six piles, the resultant force of the estimated external force was 295 N and 480 N, respectively, compared to the loaded load 630 N, resulting in a large difference between them. In addition, the resultant force of the estimated external force obviously became smaller than the loading force. From these results, in the case where the pile center distance is wide, not all external forces from the caisson act on the pile, but the external force acting between the pile and the pile, passes to the inside of the port and resisted by the ground. Looking at the external force acting on one pile, the resultant force of the estimated external force was 98.3, 80.0, and 59.6 N at 3, 6, and 12 piles, respectively. From this, it was found that the external force acting per pile is increased by widening the center to center of piles.

In the case of 12 piles, the estimation accuracy was also confirmed for some load levels. **Fig. 14** shows the subgrade reaction distribution acting on one pile at some load levels with 12 piles. This is based on the deflection distribution obtained from the bending moment distribution obtained from an experiment by the second order integration and dividing by the flexural rigidity EI of the pile and the coefficient of subgrade reaction as shown in **Fig. 11** by applying the PHRI method of type S model. **Fig. 15** shows the load distribution acting on one pile at some load levels with 12 piles, which is obtained from second-order differentiation of the bending moment distribution obtained in the experiment.

The external force distribution from the caisson side acting on one pile found by subtracting the ground reaction force distribution in **Fig. 14** and the load distribution in **Fig. 15** is shown in **Fig. 16**. Looking at the distribution of external force, it is understood that the

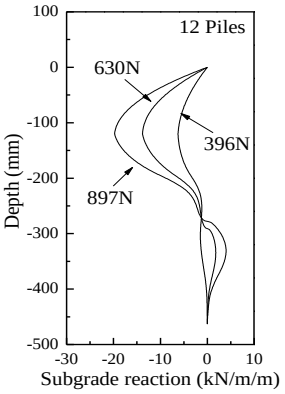

Fig. 14 Subgrade reaction distribution for the load level. (12 piles.)

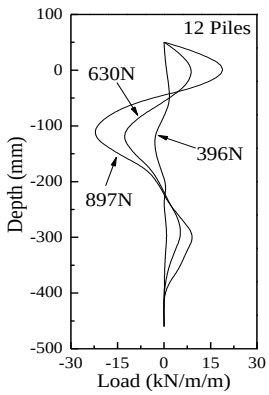

Fig. 15 Load distribution for the load level. (12 piles.)

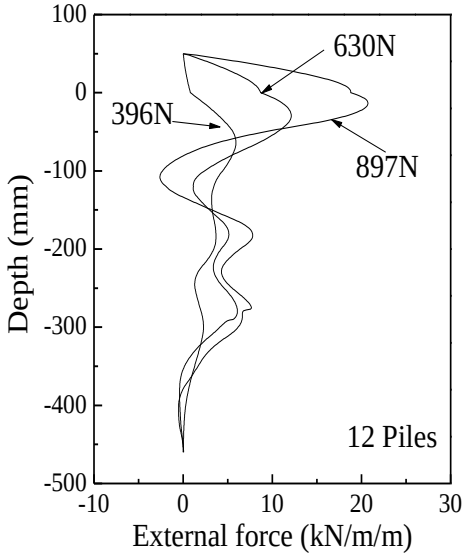

Fig. 16 External force distribution for the load level. (12 piles.)

external force does not act in the backfilling portion of 50 mm to 0 mm at the loading level of 396 N, which is the early stage of loading, and it acts in the ground. The reason may be the influence of the lateral acting force generated by the weight of the caisson and the friction of the caisson's bottom. At the loading level of 630 N, an external force acted on at the depth of 50 to -100 mm. It is considered that this external force was generated as the caisson moved and the backfilling portion was compressed. When the loading load is 897 N, the external force generated in the ground was almost the same as 630 N, but the external force generated in the vicinity of the backfilling portion dominated.

In order to investigate the validity of the estimated external force distribution, the resultant force of the

Table 4. Ratio of the resultant force of external force and loading force. (12 piles.)

①Loading force (N)	②Resultant force of the external force (N)	②/①×100 (%)
396	413	104
630	715	113
897	945	105

external force distribution acting on all the piles estimated as the loading levels were compared (**Table 4**). Since the external force distribution shown in **Fig. 15** is the external force distribution of a pile in the center, the resultant force of the external force multiplied by the number of piles was used. As can be seen from **Table 3**, since the difference between the load force and the resultant force of external forces estimated was error of 4~13%, it can be concluded that the external force can be estimated with relatively good accuracy even at the load level. The bending moment distribution acting in the pile when changing the external force distribution shape was considered. **Fig. 17** shows the external force distribution used for calculation. It is indicated by a solid black line with reference to the external force distribution of three piles in **Fig. 13**. The blue solid line is the case where the external force distribution is not applied at a depth of more than -60 mm. The red solid line is the case where the external force in the vicinity of the backfilling part (depth 50 mm to - 50 mm) is increased.

The bending moment distribution obtained is shown in **Fig. 18**. Looking at the black solid line and the blue solid line, it can be seen that the bending moment generated in the pile hardly changed, although the external force at the depth of -60 mm or more was not applied at the blue solid line. From this, it can be seen that the external force occurring at the deeper point hardly influences the bending moment distribution shape generated in the pile. Next, looking at the black solid line and the red solid line, it can be seen that the bending moment generated in the pile is larger in the red solid line with the larger external force acting near the back filled portion. From this, it was found that the bending moment distribution generated in the pile can be estimated with relatively high accuracy by considering the external force in the vicinity of the backfilling part.

Above all, the subgrade reaction acting on the steel piles acting on the passive side of the pile has been assumed and investigated using the PHRI method of type

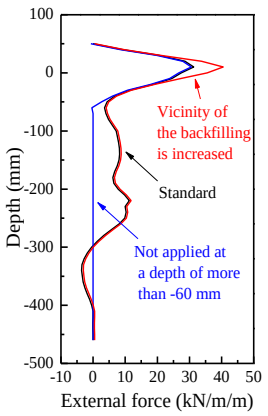

Fig. 17 Changing the external force distribution

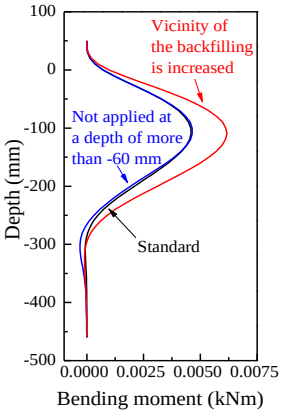

Fig. 18 Bending moment distribution

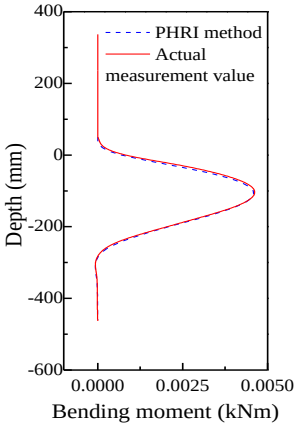

Fig. 19 Comparison of bending moment distribution of actual measurement value and calculated value.

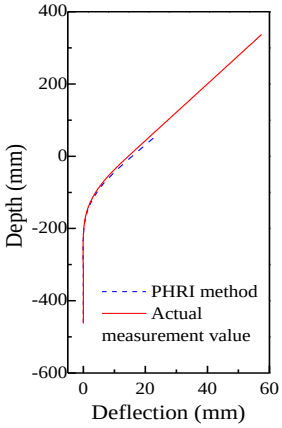

Fig. 20 Comparison of deflection distributions of actual measurement value and calculated value.

S model. However, when using this model, it is necessary to confirm whether the behavior of the actual pile can be expressed. Therefore, the inverse analysis was carried out on the validity of the PHRI method of type S model using the calculation program similar to the previous examination. **Fig. 19** shows the bending moment distribution of three piles in **Fig. 5** and the bending moment distribution obtained by inputting the reference external force in **Fig. 17** in the calculation program. **Fig. 20** shows the deflection distribution by the same comparison. Looking at these, it is understood that the bending moment and the deflection distribution coincide very well between the two. In the case of other pile conditions and loading levels, calculation of above mentioned procedure was conducted and the results

showed good agreement with this conclusion. From this, it was confirmed that the actual behavior of the pile can be represented by using the PHRI method of type S model.

4. Conclusions

In this study, the authors examined the difference of external forces received from the caisson side when changing the number of piles to be placed on the ground behind the caissons to 3, 6, and 12, and following conclusions were obtained.

1) Using the PHRI method of type S model, the ground reaction force distribution was obtained by changing k_s at the depth of maximum bending moment generation depth $l_{m, max}$, and as a result of estimating the external force distribution, in the 12 cases, the external force estimated as the load The difference of the resultant force was about 4~13%, and it was estimated with high accuracy. In the case of 3 or 6 piles, the resultant force of the external force is much lower than the loading force, not all the external forces from the caisson are transmitted to the pile, but the external force acting between the piles is inside the port. It is thought that it has become resistance in the ground by slipping through.
2) When the number of piles is changed to 3, 6, and 12, the distribution of external force at the same load becomes larger as the number of piles becomes smaller near the back-fitting part, and there is not much difference in the underground part.
3) The external force at the load level acts on the pile only in the ground at the initial stage of loading. It was found that the external forces acting on the piles dominate in the vicinity of the backfilling part by gradually compressing the backfilling part by displacement of the caisson.
4) The maximum bending moment generated in the pile was not affected by the external force occurring at the deeper point, but it was found to be affected by the external force acting in the vicinity of the backfilling part.
5) When inverse analysis was carried out using the calculation method of the PHRI method of type S model, the measured value and the bending moment obtained from the calculation program are in good agreement, and by using the PHRI method of type S model, the behavior of the pile I could confirm that I could express it.

This series of experiments was conducted under extremely limited experimental conditions. The authors consider it is necessary to investigate the effects of important parameters such as ground condition, the filled gravel between the pile and the caisson, and so on. And the authors hope to construct design procedures for this kind of improvement.

Refferences

Moriyasu, S., Tanaka, R., Oikawa, S., Miyamoto, T., Yoshiwara, K., Kikuchi, Y., Kawabe, S. and Mizuno, R. 2013. Efforts to achieve a tough structure of tsunami measures breakwater that utilizes steel wall. 7th Nankai earthquake Shikoku region Academic Symposium. (in Japanese)

Arikawa T., Oikawa S., Moriyasu S., Okada K., Tanaka R., Mizutani T., Kikuchi Y., Yahiro A., and Shimosako K. 2015. Stability of the breakwater with steel pipe piles under tsunami overflow. Technical note of Port and Airport Research Institute, No.1298, 44. (in Japanese)

Kikuchi Y., Kawabe S., Taenaka S., and Moriyasu S. 2015. Horizontal loading experiments on reinforced gravity type breakwater with steel walls. Japanese Geotechnical Society Special Publication, 2 (35), pp. 1267-1272.

Iai, S. 1988. Similitude for Shaking Table Tests on Soil-Structure-Fluid Model in 1g Gravitational Field. Report of the port and harbour research institute, Vol. 27, No.3, pp. 3-24.

Kubo, K. 1964. A New Method for the Estimation of Lateral Resistance of Piles. Report of the port and harbour research institute, Vol. 2, No. 3, pp. 13-15.